ORIGINAL ARTICLE



Leaf relative water content at 50% stomatal conductance measured by noninvasive NMR is linked to climate of origin in nine species of eucalypt

Correspondence

David Coleman

Email: David.coleman@sydney.edu.au

Abstract

Stomata are the gatekeepers of plant water use and must quickly respond to changes in plant water status to ensure plant survival under fluctuating environmental conditions. The mechanism for their closure is highly sensitive to disturbances in leaf water status, which makes isolating their response to declining water content difficult to characterise and to compare responses among species. Using a small-scale non-destructive nuclear magnetic resonance spectrometer as a leaf water content sensor, we measure the stomatal response to rapid induction of water deficit in the leaves of nine species of eucalypt from contrasting climates. We found a strong linear correlation between relative water content at 50% stomatal conductance (RWC_{gs50}) and mean annual temperature at the climate of origin of each species. We also show evidence for stomata to maintain control over water loss well below turgor loss point in species adapted to warmer climates and secondary increases in stomatal conductance despite declining water content. We propose that RWC_{gs50} is a promising trait to guide future investigations comparing stomatal responses to water deficit. It may provide a useful phenotyping trait to delineate tolerance and adaption to hot temperatures and high leaf-to-air vapour pressure deficits.

KEYWORDS

Eucalyptus, leaf water relations, physiological adaptation, stomatal response, water availability

1 | INTRODUCTION

All land plants require a continuous supply of water to replace that lost through transpiration to facilitate evaporative cooling and growth. Leaf characteristics that regulate water use and water loss over a plant's lifetime are therefore highly selective traits that allow them to persist and thrive in different environments (Sack &

Holbrook, 2006; Sack & Tyree, 2005). These traits can be macroscopic, such as leaf size, leaf shape, leaf margin or cuticle thickness (Edwards et al., 2000) or microscopic, such as those associated with hydraulic connectivity, including xylem anatomy, aquaporins, carbon pathway metabolism and stomatal dimensions (Buckley et al., 2015; Zwieniecki et al., 2007). In contrast to these semipermanent leaf traits, control of the stomatal pore aperture is

This is an open access article under the terms of the Creative Commons Attribution-NonCommercial License, which permits use, distribution and reproduction in any medium, provided the original work is properly cited and is not used for commercial purposes.

© 2023 The Authors. *Plant, Cell & Environment* published by John Wiley & Sons Ltd.

¹School of Life, Earth and Environmental Sciences, Faculty of Science, The University of Sydney, Sydney, New South Wales, Australia

²Institute for Bio-Geosciences, Juelich, Germany

³Department of Plant Sciences, University of California, Davis, California, USA

the dominant mechanism by which plants can respond rapidly to plant water status and environmental stimuli. The dynamic opening and closure of stomatal pores works in concert with other fixed leaf traits to promote the long-term survival of the organism. The relationship between stomatal responses and leaf hydraulic status is particularly important to trees and other woody species due to their large size and relatively long life cycle. However, due to methodological constraints, such as the difficulty in monitoring leaf water content within a sealed leaf gas exchange chamber and exposing the leaf to light conditions, these processes have not commonly been studied continuously and simultaneously in the same leaf (Albasha et al., 2019; Browne et al., 2020; Gente et al., 2018; Jin et al., 2017).

The genus Eucalyptus is a diverse group of woody angiosperms [more than 800 species (Thornhill et al., 2019)] in which speciation has been strongly driven by water availability across the many arid and variable climate regions of Australia (Merchant, 2014). This has given rise to a diverse range of adaptations in leaf traits across the genus, including variation in hydraulic metrics such as leaf venation morphology (Warren et al., 2006), leaf hydraulic parameters (Bourne et al., 2017) and osmotic adjustment (Merchant et al., 2007). Eucalyptus has therefore been the subject of much comparative research to investigate the mechanisms used by plants to cope with variable water availability (Körner & Cochrane, 1985; Li et al., 2019; Lucani et al., 2018; White et al., 2000). In particular, the existence of species with relatively similar leaf shapes and leaf area but adapted to vastly different dynamics of water availability, makes Eucalyptus a model genus to investigate how stomata respond to changes in leaf water content. Previous studies have shown that the sensitivity of stomata to changing conditions has been found to vary across the Eucalyptus genus, with some species responding more quickly than others to changes in leaf water status (Li et al., 2019; White et al., 2000).

The concept of stomatal 'sensitivity' is loosely adopted and rarely defined. The emerging standard measure to quantify the dynamics of changes in stomatal aperture is the bulk leaf water potential (Ψ) at 50% stomatal conductance (Ψ_{gs50}) detected over a gradient of increasing hydraulic stress (Blackman et al., 2009; Scoffoni et al., 2018). Research comparing eucalypt species has found stomatal responses to be related to hydraulic status at the whole plant level, showing that stomatal closure cooccurs with thresholds of stem water potential and loss of stem hydraulic conductance. For example, species can be compared by their theoretical 'hydraulic safety margin' given by the difference between water potential from Ψ_{gs50} and 50% loss of stem conductivity due to cavitation (P50) (Li et al., 2018). There is also evidence that the rate of leaf hydraulic conductance (K_{leaf}) is correlated with how rapidly and at what point stomata close (Scoffoni & Sack, 2017; Trueba et al., 2019). Although the hydraulic system at the whole tree level undoubtedly coordinates leaf stomatal closure via hydraulic decline, we still lack a mechanistic understanding of how stomata sense and respond to their immediate hydraulic environment.

Although stomata eventually close in response to water deficit to delay further water loss from leaf tissues, any sudden decrease in leaf hydraulic status causes a transient increase (lasting seconds to tens of minutes) in stomatal aperture called the wrong-way response (WWR)

[the WWR that occurs in response to leaf excision is sometimes called the Ivanoff effect (Ivanoff, 1928)]. As turgor pressure in the epidermal cells surrounding stomatal guard cells gives way, the stomata open, until the solute concentration of the guard cell cytoplasm can readjust to the new conditions. The stomata can then close and the conductance returns to a new equilibrium appropriate to the new hydraulic status of the leaf. Although there is evidence for rapid localised production of ABA to modulate the unloading of solutes and stomatal closure (Huber et al., 2019), the exact location and mechanisms that allow stomata to sense the hydraulic status of the leaf are still largely unknown (Buckley, 2019).

The lack of mechanistic knowledge regarding stomatal sensitivity is due in part to methodological limitations of measuring what is a highly sensitive and complex system. Standard sampling techniques used to assess leaf water status such as the Scholander pressure chamber (water potential), psychrometry (water potential) or gravimetric analysis (water content), normally require destructive sampling, which interrupts the natural transpiration pathways and potentially damages leaf tissue (Browne et al., 2020; Scoffoni & Sack, 2017). To assess both stomatal conductance and hydraulic status, several leaves must be assumed to behave identically to the same treatment (Sack & Scoffoni, 2012). The natural spatial heterogeneity of leaf anatomy and rate of physiological responses (Fahn & Broido-Altman, 1990; Hernandez-Santana et al., 2016) thus reduces the sensitivity and precision of measurements.

Nuclear magnetic resonance (NMR) relaxometry, also known as time domain NMR (TD-NMR), can be used to measure the water content of living samples directly and non-destructively (Van As, 2006) and does not interfere with the hydraulic system of plant tissues (Borisjuk et al., 2012). Conventional benchtop TD-NMR instruments have been designed to measure test tubes. Due to their narrow bore and sensitivity to changing temperatures, they typically are not well suited to measure plants. Van As et al. (1994) were the first to modify such an instrument to allow TD-NMR of plant water status in a greenhouse setting (Van As et al., 1994). More recently. rapid developments in magnet materials, wireless communication technologies and processing power of mobile devices enabled the development of powerful yet mobile, low-field, small scale NMR devices for the plant sciences (Windt et al., 2011, 2021) that can be used in the greenhouse or field. Combined with a novel relaxometric method [solid liquid content determination (SLC)], such devices can be used in a sensor-like manner to instantaneously and noninvasively measure fresh weight, water content and dry matter content in living plants (Windt et al., 2021). So far, such NMR plant sensors have been applied to monitor dynamic changes in the water content of stems (Lechthaler et al., 2016; Windt & Blumler, 2015), fruit and leaves (Lechthaler et al., 2016) as well as dry matter deposition in developing seeds (Merchant et al., 2022; Windt et al., 2021). In the current study, we integrate a custom-built transparent gas exchange cuvette into the NMR sensor. Attached to a standard gas exchange measurement system, this novel setup allows to simultaneously and non-destructively monitor the water status of illuminated, intact and functioning leaves.



Using NMR sensing in conjunction with existing gas exchange measurement techniques, we characterised stomatal responses to bulk leaf hydraulic status across a range of eucalypt species to evaluate their potential adaptive advantage to their native climates. We simultaneously measured the g_s and water content of leaves subjected to consistent light conditions over an experimental dry down from nine species of eucalypt, obtained from a range of climates across Australia and grown in a common botanic garden setting. We tested the validity of the combined NMR sensor and infra-red gas analyser (IRGA) apparatus in monitoring hydraulic status and stomatal function as well as the resilience of stomatal control to the dry down treatment among eucalypt species. We determined at what RWC stomatal closure was achieved and tested whether this could be linked to other leaf hydraulic traits such as RWC_{TLP}. We further test the hypothesis that metrics such as leaf RWC at the end of the WWR and RWC at RWC₉₅₅₀ differ between species and correlate with climate of origin variables.

MATERIALS AND METHODS

Site characteristics

Nine species of eucalypt originating from a broad taxonomic scope were analysed. Seven different Sections were represented, six of which reside within the most diverse Eucalyptus subgenus: Symphyomyrtus (Table 1). Such species originated from a broad range of climates (Table 1). Of particular note is mean annual temperature (MAT) of seed locations between 13.2°C for Eucalyptus laevopinea and 23.5°C for Corymbia tessellaris and mean annual precipitation (MAP) between 1335 mm for Eucalyptus grandis and 350 mm for Eucalyptus caesia.

All plant material was sourced between mid-June to mid-August 2020 from the Mount Annan Botanic Gardens (34° 4'13" S. 150°46′12" E, elevation 150 m). The site has a MAT of 16.5°C and MAP of 780 mm. During the 6 months before the experiment, the site experienced temperatures close to the long-term average (average daily maximums ~30-20°C minimums 20-10°C) but almost double the longterm average rainfall (566 and 295 mm, respectively). Temperatures and rainfall during the experiment were similar to the long-term average with daily average maximum and minimum temperatures of 17-18°C and 3-5°C respectively, and ~100 mm rainfall over the 2.5 months. The Mount Annan Botanic Gardens soils are dominated by well-drained Kurosols and Dermosols. Seed progeny data was provided by the Mount Annan Botanic Gardens (Table 1). Climate data for species were sourced from the Atlas of Living Australia Spatial Portal (http://spatial. ala.org.au/; accessed 6 October 2020).

2.2 Sample collection

Each morning of the experiment, one small branch (~30 cm) of adult foliage was cut from mature trees (>5 years old) using clean, sanitised

secateurs. Sampled branches were always situated on a light exposed, north or east facing side of the tree. The branch was immediately recut under water, covered and transported (20 min) by car to a laboratory at the Centre for Carbon Water and Food, The University of Sydney. The branch was then placed in a dark cupboard to rehydrate and leaf surfaces dried with a tissue if necessary, until the time of measurement (1.5-2 h from the time of harvest), at which point it was confirmed whether full turgor in the branch had been reached using a Scholander pressure chamber (Model 1505D; PMS Instrument Company).

Measurement of leaf RWC using the NMR 2.3 sensor

To simultaneously measure leaf gas exchange and leaf RWC, a mobile NMR sensor was fitted with a glass cuvette connected to an IRGA. The continuous, non-destructive measurement of proton density of the liquid fraction inside the leaf was undertaken using an NMR sensor as described by Lechthaler et al. (2016). The sensor consists of a C-shaped, temperature stable permanent magnet with a field strength of 0.235 T (¹H Larmor frequency 10 MHz) over an air gap of 37 mm. It was fitted with a 12-turn, 15 mm diameter solenoidal radio frequency (RF) coil of 20 mm in height, wrapped around the narrow section of the gas exchange cuvette (Figure 1). The NMR sensor was driven with a standard KEA II spectrometer (Magritek) with a built-in 350 W RF amplifier. The spectrometer was housed in an insulated, temperature-regulated aluminium case, set to a constant temperature of 40°C (±1°C). The spectrometer was controlled using the proprietary software (Prospa v3.21: Magritek) on a laptop running Windows. Liquid proton density (PD_{lia}) was measured and quantified using the SLC approach as described by Windt et al. (2021). For the SLC determination an FID-CPMG sequence was run with the following experimental settings: Inter-experimental time (repetition time) 1 s; repetitions 32; number of echoes: 50; echo time: 500 ms; spectral width: 1 MHz; 90° pulse: 3-3.25 µs/-6 dB; 180° pulses: $10.5-11.25 \,\mu s/-12 \,dB$.

Connection of the IRGA to the NMR cuvette

Inlet and outlet tubes connected the cuvette to an IRGA (LI-6400XT; LI-COR, Inc.). These tubes were ~30 cm in length to ensure minimal lag time between the air exiting the cuvette and entering the IRGA sample cell. The gas inlet, outlet and leaf temperature thermocouple were inserted into the leaf cuvette through a moulded-for-purpose silicone rubber stopper at the base of the cuvette (Figure 1). To avoid transmission of external RF noise into the NMR sensor the thermocouple was placed as far away from the RF coil as possible, at ~2 cm from the base of the cuvette, close to but not touching the leaf and shaded from the external light source. At the opposite end of the cuvette, a second stopper closed around the leaf petiole and any air leaks were sealed using silicone gel vacuum grease (Figure 1). The

Taxonomy (Thornhill et al., 2019), section climate of origin description (Boland et al., 2006) and climate variables (sourced from Atlas of Living Australia) for nine species of eucalypt. TABLE 1

Species	Genus	Subgenus	Section (no. species)	Common name groupings	Section climate range	MAP (mm)	MAT (°C)	MARH (%)
Angophora crassifolia	Angophora	Angophora Angophora	Angophora (10)	Appleboxes	East coast of Australia extending from cooler high rainfall regions to warmer, semiarid inland SQL	1233	17.5	72.04
Corymbia tessellaris	Corymbia	Blakella	Abbreviatae (19)	Paper-fruited bloodwoods	Absent from the winter rainfall areas but show a wide tolerance in tropical and subtropical regions	981	23.5	68.94
Eucalyptus atrata	Eucalyptus	Eucalyptus Symphyomyrtus Adnataria (106)	Adnataria (106)	Boxes and Ironbarks	Boxes and Ironbarks Widely distributed outside truly arid regions in areas of moderate to high rainfall	881	21.1	67.5
Eucalyptus caesia	Eucalyptus	Eucalyptus Symphyomyrtus Bisectae (126)	Bisectae (126)	Mallees and Mallets	See E. macrandra. Exclusive occurrence of this species on isolated granite rocks in semiarid regions of WA	350	18.2	57.21
Eucalyptus grandis		Symphyomyrtus	Eucalyptus Symphyomyrtus Latoangulatae (22)	Mahoganies	Confined to the coastal strip of E. Australia to PNG in high rainfall areas	1335	20	69.71
Eucalyptus laevopinea	Eucalyptus	Eucalyptus Eucalyptus	Eucalyptus (99)	Stringybarks	Species of cool, moist climates. Annual rainfall 100–1500 distributed throughout the year	904	13.2	71.03
Eucalyptus Iongifolia	Eucalyptus	Eucalyptus Symphyomyrtus Incognitae (3)	Incognitae (3)		Central and southern coastal forests of NSW, not closely related to any other species in the genus	006	17.7	70.15
Eucalyptus macrandra	Eucalyptus	Eucalyptus Symphyomyrtus Bisectae (126)	Bisectae (126)	Mallees and Mallets	Centre of section speciation is in SW WA in Mediterranean to semiarid climates	503	16.2	72.47
Eucalyptus tereticornis	Eucalyptus	Eucalyptus Symphyomyrtus Exsertaria (45)	Exsertaria (45)	Eastern Redgums	Has the most extensive latitudinal distribution of the genus, extending from coastal south-eastern VIC to southern PNG. In drier areas, prefers alluvial flats subject to occasional flooding	1122	15.7	72.75

Abbreviations: MAP, mean annual precipitation; MARH, mean annual relative humidities; MAT, mean annual temperature.

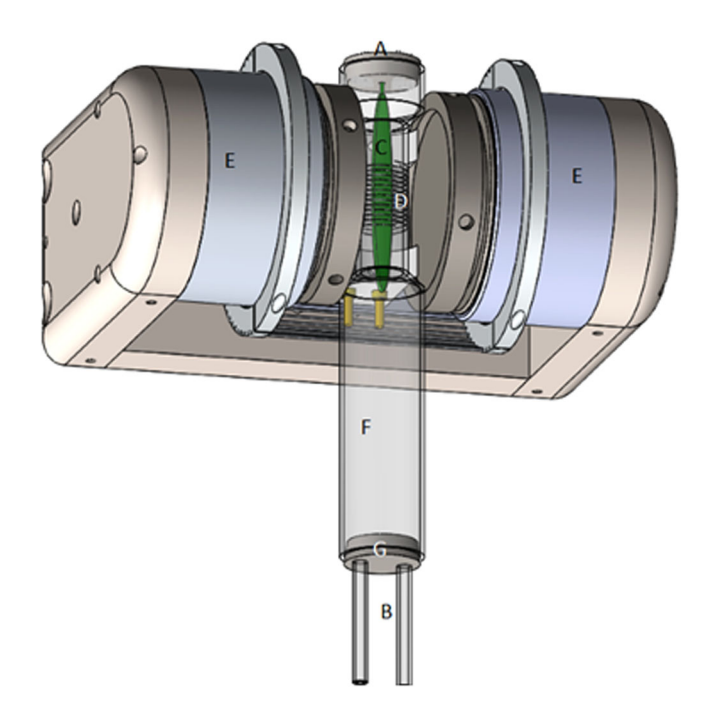


FIGURE 1 Adapted design for the sealed glass cuvette/coil housing for the NMR. (A) Silicon rubber stopper sealed around the petiole of the leaf connected to a branch, (B) the gas inlets and outlets connecting the chamber to the IRGA, (C) intact leaf connected to a branch, (D) the wire coil surrounding the leaf, (E) NMR magnets, (F) large space the coil to accommodate longer leaves and facilitate mixing of gases, (G) a second silicon rubber stopper sealing the gas inlets and outlets. IRGA, infra-red gas analyser; NMR, nuclear magnetic resonance.

strong magnetic field in the NMR magnet prohibited the use of gas mixing fans inside the cuvette. Adequate mixing of gas could however be ensured by judicious placement of the inlet tubes and was confirmed by observing the stability of the differential between sample and reference H₂O concentrations with a transpiring leaf placed in the cuvette.

Measurements of gas exchange and leaf water status during leaf desiccation

For the nine eucalypt species, within each branch chosen for the dry down procedure a healthy, fully expanded leaf was selected. While still attached to the hydrated branch and the cut stem held in a beaker of water, the leaf was photographed for calculation of leaf area and placed in the NMR sensor/IRGA cuvette. The IRGA and NMR sensor logged continuously every 3 and 2 min, respectively, for the remainder of the experiment. Once sealed inside the cuvette, the leaf remained in dim light conditions [$<10 \,\mu mol m^{-2} s^{-1}$] photosynthetically active radiation (PAR) for ≥20 min until g_s was stable, changing no more than 0.01 mol m⁻² s² (from IRGA) and PD_{lia} was stable to within 1% over 15 min]. The branch was then illuminated with one large and two smaller LED light panels, providing ~700 µmol m⁻² s⁻¹

PAR to the branch as well as to the leaf inside the cuvette. The leaf and branch remained in these new conditions for ≥60 min until g_s was stable again [variability <0.02 mol m⁻² s² (from IRGA) and the PD_{liq} did not vary more than 1% over 15 min]. The dry down procedure was started by removing the beaker of water from the fixed stem. The branch was then left to dry under constant light for ≥5 h, while gas exchange and RWC were continuously monitored. Following the dry down procedure, the leaf was removed from the cuvette, cut from the branch, weighed, placed in 60°C oven for 24 h and weighed again to establish the dry weight and specific leaf area (SLA).

Flow rate and CO₂ concentration inside the cuvette were controlled by the IRGA (flow = 700 μ mol s⁻¹, reference CO₂ = 400 μ mol mol⁻¹). The cuvette did not include temperature control. Leaf temperature (inferred from air temperature) ranged between 22°C and 25°C which followed small fluctuations in the lab temperature over the experiment. Leaf-to-air vapour pressure deficit (VPDL) increased from ~0.6 kPa when the leaf was in the dark to ~0.9 kPa during the initial few hours in the light, it then steadily increased as the leaf dried to ~1.5 kPa. The reference and sample lines of the IRGA were matched immediately before each measurement, every 3 min.

Calibration of liquid proton density against leaf water weight

Reference curves to establish the linear relationship between leaf water weight (WW_{leaf}) and the liquid proton density (PD_{liq}) as measured by the NMR sensor were constructed as per the SLC method (Windt et al., 2021). Leaves were severed from well hydrated branches and either measured immediately with the NMR sensor, or left to bench dry for increasing periods of time before measuring. Each leaf thus represents one data point on the curve (Figure 3a). Leaves that were wider than the neck of the cuvette with the RF coil were gently rolled up before insertion. The sensitive volume of the NMR sensor is determined by the dimensions the RF coil hat is used, here 15 mm in diameter and 20 mm in height. After NMR measurement the length of leaf inside the sensitive volume of the NMR RF coil was marked, the 20 mm length of leaf that sat in the RF coil excised with a scalpel, and water weight determined gravimetrically. To this end samples were weighed, oven dried overnight at 60°C and reweighed. Sample WW was determined by subtracting their dry weights from their fresh weights. WW was then plotted against PD_{liq} for the samples of the various species and fitted with a linear regression:

$$WW = \beta_0 + \beta_1 PD_{lia}$$
 (1)

Definition 100% leaf RWC 2.7

During the branch dry down experiments leaf RWC was defined as the ratio between the instantaneous and the maximum water weight (in grams) in same section of leaf tissue inside the coil as measured by the NMR sensor. The RWC, expressed as a percentage, during the dry down of the leaf was then calculated as:

emed by the applicable Creative

$$RWC = \frac{WW}{WW_{max}} \times 100$$
 (2)

where WW is the instantaneous leaf water weight and WW_{max} is the leaf water weight at full turgor.

2.8 | Assessing the agreement between IRGA and NMR

Four branches of *Eucalyptus tereticornis* were hydrated and loaded into the cuvette and dried down under light conditions in the same way as the experimental method outlined above, but water supply was terminated by severing the leaf at the petiole rather than by removal the water supply of the branch. Without water input to the leaf, the cumulative weight of water transpired, expressed in terms of leaf RWC (measured by the IRGA) should equal the decrease in leaf RWC registered by the NMR. An estimate of 100% RWC for the entire leaf (necessary for the calculation of RWC by the IRGA) was inferred from the average ratio of fresh weight (g) to the SLA (kg m⁻²) of five similar sized leaves from the same branch. Thus, the data output from the two technologies could be represented graphically using the same unit (RWC).

2.9 Leaf hydraulic traits and leaf area

Five comparable leaves from the same branch were harvested, photographed and their area calculated in Rstudio (Team RStudio, 2015) using the EBImage package (Pau et al., 2010), weighed and placed in a 60°C oven and weighed again to calculate an average SLA for that branch. Each leaf that was monitored over the drydown by the two technologies had its SLA calculated in a similar way, with the photograph of the leaf being taken before loading into the cuvette while still attached to the branch and the dry weight determined at the end of the dry-down.

Stomatal leaf peels were obtained from one leaf per branch using nail polish and placed onto a microscope slide using sticky tape and photographed at ×100 magnification on a LEICA DFC 500 digital camera on a LEICA DM 2500 LED optical microscope for stomatal density and size. The stomatal length and number were measured and counted using ImageJ software (Schindelin et al., 2012). The stomatal density was determined from the number of stomata visible per 1.8 mm² field of view of the image, while the mean stomatal length per side was determined from the average of 10 stomatal pore lengths. The stomatal pore index (SPI) was used as a summary trait to describe stomatal anatomy and calculated as proposed by Sack et al. (2003) as follows:

SPI =
$$(guard cell length)^2 \times stomatal density$$
 (3)

One leaf per branch from each of the same individuals was harvested, hydrated in the dark in the same way as the whole branches and used to construct pressure-volume relationships (Merchant et al., 2007; Tyree & Hammel, 1972) using a Scholander pressure chamber (Model 1505D; PMS Instrument Company) and electronic balance to 5 decimal places.

2.10 | Data processing, statistical analysis and parameterisation of dehydration curves

Data processing and analysis was conducted in Rstudio (Team RStudio, 2015). A smoothing spline using the *smooth.spline()* function from the stats v 3.6.2 package in base R (R Core Team, 2019) was fitted over the NMR sensor data to match timestamps between the NMR sensor and IRGA devices.

The magnitude of the stomatal 'WWR' that occurred following removal of the water supply, the timespan of the WWR and the g_{sinitial} were extracted from the data as shown in Figure 2. A local polynomial regression fitting *loess()* function from the stats package was fitted over the raw transpiration data to establish the first derivative of the WWR. The function cumtrapz() from the pracma package (Borchers & Borchers, 2019) was used to calculate the amount of water lost during the WWR, on the basis of the area under the transpiration curve on the time interval from removal of water at 0 s until returning to g_{sinitial} (Figure 2).

One-way ANOVA with post hoc Tukey's HSD tests were used to compare species traits using the agricolae package, v1.3-3 (de Mendiburu & de Mendiburu, 2020). Normality and homogeneity of variance were checked visually with a normal QQplot and a residuals vs fit plot from the same package. Relationships between variables were analysed with linear regression. A principal component analysis (PCA) on independent leaf morphological and physiological traits was used to test multivariate associations using the *prcomp()* function in

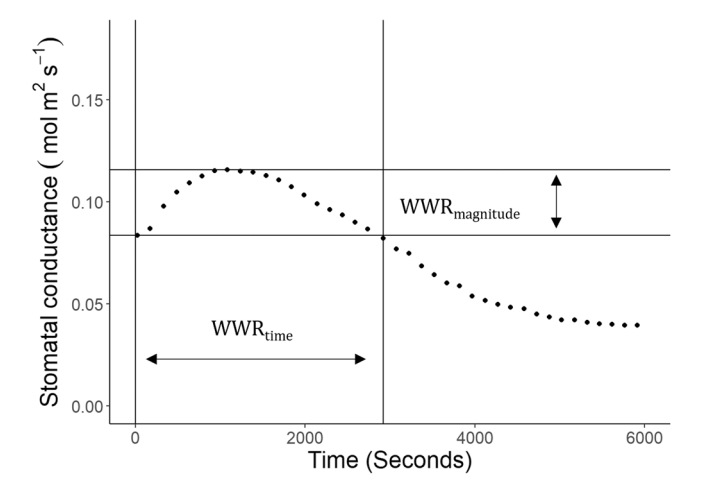


FIGURE 2 The magnitude (WWR $_{magnitude}$) and duration (WWR $_{time}$) of the stomatal WWR were extracted from the stomatal conductance curve using the maximum and initial rates of stomatal conductance as shown. WWR, wrong way response.

the stats v 3.6.2 package base R (R Core Team, 2019). Leaf traits that were selected were independent and representative of the leaf's physical and phsyiological characteristics. Plots were constructed using ggplot2 v 3.3.2, (Villanueva & Chen, 2019) with the ggbiplot (https://github.com/vqv/ggbiplot) package in R.

3 **RESULTS**

The linear relationship between water mass in leaf tissues of the nine species of eucalypt and the signal strength of the liquid proton density PD_{liq} was established via extensive calibrationover a wide range of tissue hydration and for many different leaves, for each species examined in this study. The relationship was highly significant (p < 0.001) for all species with a mean R^2 of 0.92 (Figure 3a). Furthermore, similar reference curves produced from repeatedly measuring the same leaf sample over the range of leaf tissue hydration experienced in this study produced curves with R² values that ranged from 0.990 to 0.995 (examples in Supporting Information: Figure S1). A final confirmation of how well the measurement of leaf RWC aligned with leaf transpiration was undertaken by comparing the simultaneous estimates of RWC of leaves of E. tereticornis as measured by the NMR and IRGA. The resulting two traces were closely aligned (Figure 3b). The NMR estimated leaf RWC to decline somewhat more rapidly than the IRGA in the initial stages of the drydown in most cases (Figure 3), with a maximum discrepancy of 7% RWC. Despite this deviation, in all cases the estimate of RWC from the IRGA realigned with the NMR results below ~40% RWC, following a slowing in the rate of drying as determined by NMR. Below ~20% RWC, the signal to noise ratio of the NMR estimate of PD_{liq} became too low to reliably

estimate RWC. With the NMR settings and hardware used in this study this would equates to water masses of around 0.02 g within the leaf tissue measured by the NMR.

Leaves selected for the study comprised a broad scope of leaf physical characteristics including total fresh weight, leaf area, SLA and SPI (Table 2). Of particular note is the >twofold difference in SLA from 3.00 m² kg⁻¹ (E. caesia) to 7.04 m² kg⁻¹ (C. tessellaris), a >threefold difference in SPI from 2.04 (Eucalyptus macrandra) to 7.89 (E. tereticornis) and >fourfold difference) in leaf fresh weight 0.381 g (Angophora crassifolia) to 1.61 g (E. caesia).

Dynamics of stomatal conductance during branch dehydration

For all species tested in this study, a decline in leaf RWC commenced immediately after the removal of water supply for all species, registering a >15% reduction in RWC within the first hour for most leaves (Figure 4). Following the initial rapid leaf water loss rates generally slowed. Leaves of some species such as Eucalyptus atrata and E. caesia did not decrease below 50% RWC, despite experiencing full light conditions for more than 10 h without a supply of water to the branch stem. All leaves demonstrated an initial increase in g_s following the removal of water supply from the stem, typical of a stomatal WWR. Rates of increase in gs then slowed, resulting in an eventual plateau followed by a rapid decline towards very low or negligible rates of g_s for the remainder of the dehydration.

WWR metrics of g_s including time and magnitude were not well differentiated by species, with only two post hoc classifications for each metric (Table 3). Time intervals from removal of the stem water supply to the g_{smax} (WWR_{time}) ranged from ~30 min to almost 2 h

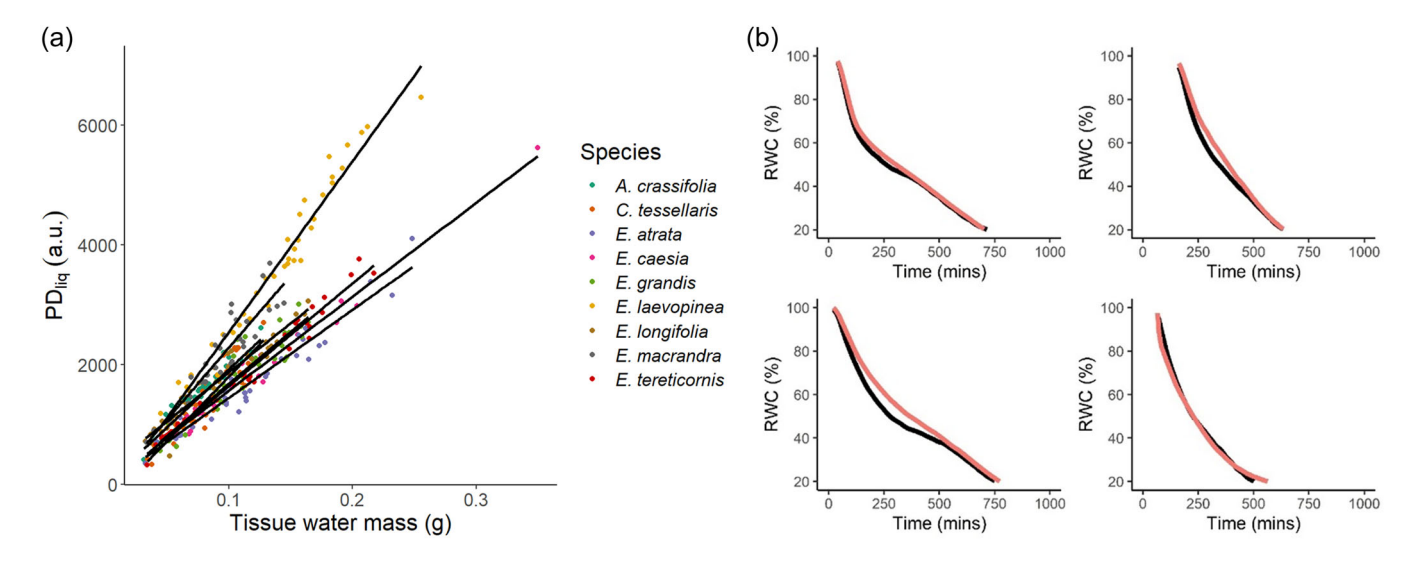


FIGURE 3 (a) NMR reference curves for leaf tissue of nine species of eucalypt. Leaves were harvested progressively from a drying branch, each data point represents a new leaf. PDiia is expressed in arbitrary units of signal amplitude (a.u.). (b) Leaf RWC of a severed leaf simultaneously estimated using data from NMR sensor (black lines) and IRGA (red lines) of four Eucalyptus tereticornis leaves exposed to high light conditions. IRGA, infra-red gas analyser; NMR, nuclear magnetic resonance. [Color figure can be viewed at wileyonlinelibrary.com]

13653040, 2023, 12, Downloaded

elibrary.wiley.com/doi/10.1111/pce.14700 by University Of California - Davis, Wiley Online Library on [23/07/2025]. See the Terms

on Wiley Online Library for

rules of use; OA articles are governed by the applicable Creative Comm

TABLE 2 The physical characteristics of leaf morphology for nine species of eucalypt.

Species	Fresh weight (g)	Leaf area (cm²)	SLA (kg m ²)	SPI × 10 ²
Angophora crassifolia	0.381 ± 0.04^{c}	14.0 ± 1.2^{c}	6.05 ± 0.41^{ab}	2.59 ± 0.4^{cd}
Corymbia tessellaris	0.577 ± 0.14 ^{bc}	$17.2 \pm 0.8a^{bc}$	7.04 ± 0.61^{a}	3.36 ± 0.7^{bcd}
Eucalyptus atrata	0.577 ± 0.08 ^{bc}	16.8 ± 0.7^{bc}	5.18 ± 0.77 ^{abc}	3.96 ± 0.4^{bcd}
Eucalyptus caesia	1.610 ± 0.16^{a}	22.3 ± 1.2 ^{ab}	3.00 ± 0.10^{c}	4.37 ± 0.5^{bcd}
Eucalyptus grandis	0.622 ± 0.03^{bc}	22.3 ± 1.5 ^{ab}	6.81 ± 0.77 ^a	5.03 ± 0.3^{bc}
Eucalyptus laevopinea	0.662 ± 0.05 ^{bc}	17.6 ± 1.3 ^{abc}	5.57 ± 0.49 ^{ab}	5.50 ± 0.9^{ab}
Eucalyptus longifolia	0.718 ± 0.05^{bc}	21.7 ± 1.8 ^{ab}	6.64 ± 0.50^{a}	3.10 ± 0.4^{bcd}
Eucalyptus macrandra	0.565 ± 0.05 ^{bc}	12.1 ± 0.9°	3.75 ± 0.11 ^{bc}	2.04 ± 0.4^{d}
Eucalyptus tereticornis	0.877 ± 0.05 ^b	24.4 ± 2.6^{a}	6.21 ± 0.68^{ab}	7.89 ± 0.6^{a}

Note: Values displayed are mean \pm SE and groupings are based on post hoc LSD test of a one-way ANOVA. Letters (a, b, c and d) represent significantly different groupings, α = 0.05, n = 4. The stomatal pore index (SPI) representing the density of stomatal pore area, is estimated from the leaf surface of an adjacent leaf.

Abbreviation: SLA, specific leaf area.

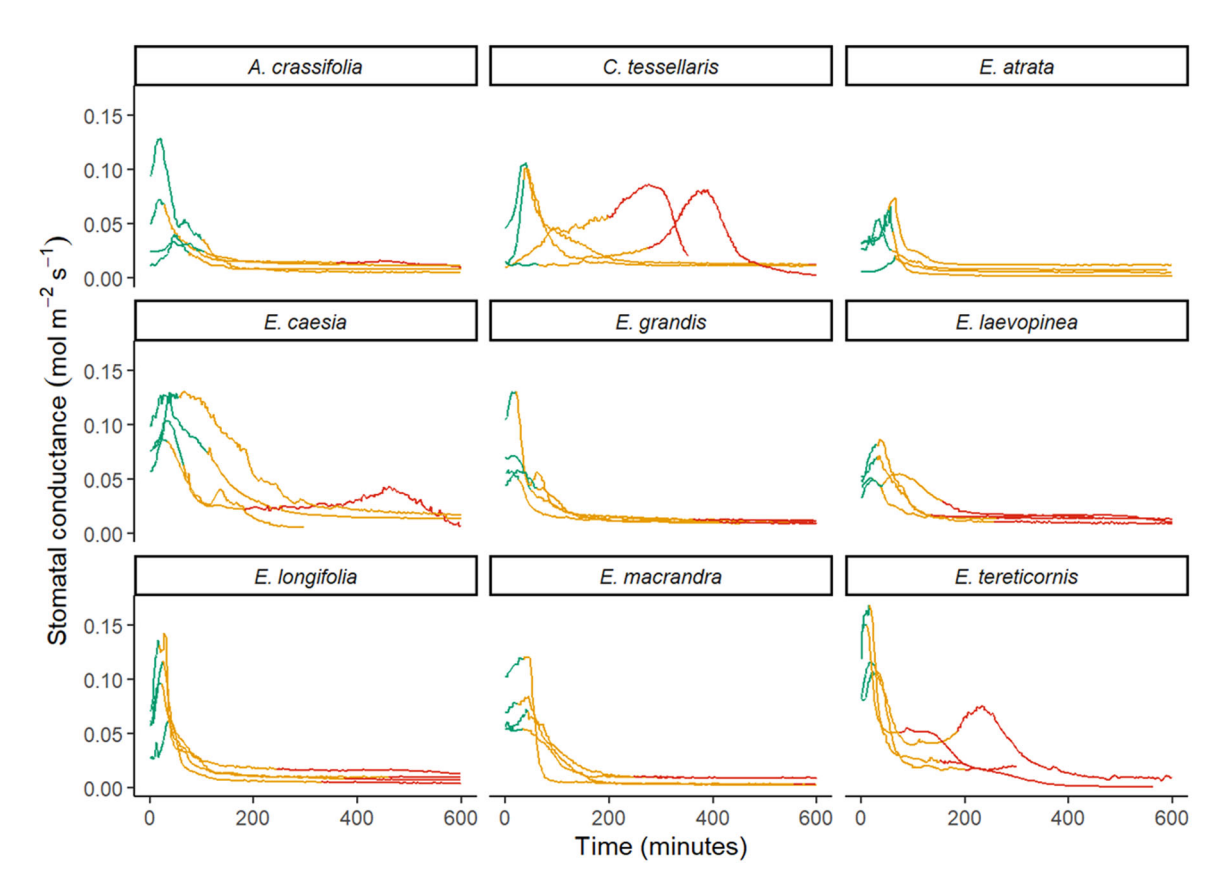


FIGURE 4 The stomatal conductance versus time for leaves of nine species of eucalypt exposed to light after stem water supply was removed. Each trace represents one leaf. Colours indicate the RWC of the leaf (green: RWC > 85%, yellow: 85% < RWC > 50% and red: RWC < 50%). [Color figure can be viewed at wileyonlinelibrary.com]

across all species (Table 3). Stomatal closure occurred in leaves of *E. grandis* and *A. crassifolia* at the highest leaf RWC, while *E. laevopinea* began closing its stomata at significantly lower RWCs than other species.

Some replicates of *C. tessellaris*, *E. tereticornis* and *E. caesia* exhibited a second increase in g_s at RWCs below 50% (Figure 4). Replicates which displayed this response were therefore excluded from analyses of data during the latter stages of leaf desiccation.



TABLE 3 The metrics for the stomatal conductance and wrong way response (WWR) of nine species of eucalypt.

Species	$g_{\rm s\ initial}$ (mol m ² s ⁻¹)	WWR _{time} (min)	RWC _{WWR} (%)	WWR _{magnitude} (mol m ² s ⁻¹)
Angophora crassifolia	0.035 ± 0.01^{b}	78 ± 24a ^b	90.3 ± 1.0 ^a	0.019 ± 0.005^{ab}
Corymbia tessellaris	0.021 ± 0.01 ^b	117 ± 27^{a}	80.3 ± 4.1^{ab}	0.051 ± 0.016^{a}
Eucalyptus atrata	0.024 ± 0.01^{b}	75 ± 11 ^{ab}	84.7 ± 2.2 ^{ab}	0.028 ± 0.006^{ab}
Eucalyptus caesia	$0.076 \pm 0.01a^b$	89 ± 25 ^{ab}	87.1 ± 2.3 ^{ab}	0.033 ± 0.013^{ab}
Eucalyptus grandis	0.066 ± 0.01^{ab}	30 ± 3^{b}	90.1 ± 2^{a}	0.009 ± 0.005 ^b
Eucalyptus laevopinea	0.043 ± 0.01 ^b	72 ± 16 ^{ab}	76.4 ± 3.7 ^b	0.020 ± 0.005^{ab}
Eucalyptus longifolia	0.054 ± 0.01^{ab}	43 ± 5^{ab}	78.6 ± 2.3^{ab}	$0.046 \pm 0.006_a$
Eucalyptus macrandra	0.070 ± 0.02^{ab}	55 ± 7 ^{ab}	78.4 ± 3.6 ^{ab}	0.013 ± 0.005 ^b
Eucalyptus tereticornis	0.103 ± 0.01^{a}	36 ± 6^{b}	83.3 ± 1.9 ^{ab}	0.028 ± 0.002^{ab}

Note: Values displayed are mean ± SE and groupings based on post hoc LSD test of a one-way ANOVA. Letters (a and b) represent significantly different groupings, $\alpha = 0.05$, n = 4.

Abbreviations: ge initial, the initial rate of stomatal conductance of a leaf under stable hydraulic state and light conditions; RWC_{WWR}, the RWC following the WWR; WWR_{magnitude}, the maximum increase in gs observed over the WWR; WWR_{time}, the time taken for the stomatal conductance to return to gs_{initial}.

Pressure-volume (PV) derived hydraulic parameters and RWC at g_s50 of species of leaves of nine species of eucalypt.

Species	RWC _{TLP} (%)	Ψ _{TLP} (MPa)	π _{FT} (MPa)	ε	RWC _{gs50} (%)
Angophora crassifolia	88.14	-2.74	-2.65	25.03	82.1 ± 1.9 ^a
Corymbia tessellaris	93.85	-2.39	-1.93	43.30	-
Eucalyptus atrata	95.71	-1.61	-1.36	24.67	81.8 ± 1.8^{a}
Eucalyptus caesia	94.71	-2.10	-1.97	36.63	76.4 ± 4.3^{ab}
Eucalyptus grandis	90.82	-2.11	-1.80	31.51	80.4 ± 1.7^{ab}
Eucalyptus laevopinea	90.76	-2.38	-2.05	24.39	$61.4 \pm 4.7^{\circ}$
Eucalyptus longifolia	90.37	-2.36	-2.30	25.22	71.3 ± 1.2^{abc}
Eucalyptus macrandra	91.84	-2.66	-2.64	36.55	68.3 ± 2.8^{bc}
Eucalyptus tereticornis	92.46	-2.63	-2.40	43.41	67.6 ± 0.3^{bc}

Note: PV parameters are derived from one relationship using data of leaves from four individuals. The RWC at gs50 parameter is the mean and SE of each species, with post hoc groupings a, b and c representing significant differences ($\alpha = 0.05$). It was not possible to calculate RWC_{gs50} for C. tessellaris. Abbreviations: RWC_{TLP}, the bulk RWC at turgor loss point; Ψ_{TLP} , the bulk leaf water potential at turgor loss point; π_{FT} , the leaf osmotic potential at full turgor; E, the bulk elastic modulus of leaf tissue between full turgor.

Measured and derived physiological parameters significantly differ among species (post-WWR)

We hypothesised that metrics describing stomatal closure, such as the RWC loss during the WWR (RWC_{WWR}) and RWC at RWC_{gs50}, would correlate with hydraulically significant parameters in the leaf such as RWC_{TLP}. Surprisingly, RWC_{WWR} was much lower than the RWC_{TLP} for most species (Tables 3 and 4); that is, the amount of water lost during the WWR-before g_s had declined even to its initial value-was more than enough to reduce leaf turgor to zero, even if the leaf initially was fully hydrated. Similar to the WWR metrics, the RWC_{TLP} was relatively consistent between species, with eight of the species lying between

90% and 95%, as was the spread of water potential parameters [-1.61 to $-2.66\,\text{MPa}$ water potential at turgor loss point (Ψ_{TLP}), $-1.36\,$ to -2.64 MPa osmotic potential at full turgor (π_{FT})]. Furthermore, neither the species ranking of RWC_{TLP} nor the Ψ_{TLP} correlate with the magnitude or length of the WWR. RWC_{gs50} used here as a representation of stomatal closure and sensitivity, occurred well below the RWC_{TLP} in all species [up to ~30% lower in E. laevopinea leaves and could be grouped into three significantly different cohorts (Table 4)]. Leaf tissues of C. tessellaris, E. tereticornis, E. caesia, E. macranda had a higher bulk elastic modulus (ɛ) than other species, showing a greater decline in water potential per unit decrease in RWC before turgor loss. Three of the four species mentioned here exhibited secondary increases in g_s as mentioned previously.

.3653040, 2023, 12, Downloaded from https

nelibrary.wiley.com/doi/10.1111/pce.14700 by University Of California - Davis, Wiley Online Library on [23/07/2025]. See the Terms

on Wiley Online Library for rules of use; OA articles are governed by the applicable Creative Com

3800

3.3 | Relationships between physiological parameters and climates of origin

Across species, RWC_{gs50} correlated significantly with the MAT of the seed collection location; RWC_{gs50} increased by 2.71% RWC with every 1°C of MAT (R^2 : 0.85, p = 0.001; Figure 5b). The omission of A. crassifolia (a 'true eucalypt' precursor) results in an even stronger relationship (R^2 : 0.97, p < 0.001; regression not shown in Figure 5). In contrast, the MAP of seed locations was only weakly related (R^2 : 0.022, p = 0.726) (Figure 5a). A MANOVA test for the two dependent variables of MAP and MAT was highly significant (p < 0.001).

A PCA was used to analyse how variation in physiological parameters covaried with RWC_{gs50} (Figure 6). The first two components accounted for ~65% of the variation in RWC_{gs50} from the pooled data of five independent hydraulic and physiological traits of leaves. Species were evenly distributed across both axes, with the first component (PC1 40% variation explained) most associated with loadings from g_s initial and ε , while the second component (PC2 20% variation explained) was most associated with loadings from PV curve derived parameters and SPI.

4 | DISCUSSION

We analysed the response of g_s to changing RWC of nine eucalypt species originating from contrasting climates using a novel combination of NMR sensing and simultaneous leaf gas exchange analysis. The dynamics of leaf responses to leaf dehydration, coupled with traditional measures

of leaf biochemical and biophysical properties illustrate the strong association of water management properties on the speciation of *Eucalyptus* in response to increasingly arid conditions. Species can be differentiated by the ability of leaves to cope with extreme hydraulic stress, with parameters such as RWC_{gs50} correlating strongly with parameters delineating environmental origin.

Combining NMR with leaf gas exchange measured by IRGA, provides significant advantages for the non-destructive measurement of water flow through plant tissues. For the first time, both water flux and RWC have been measured simultaneously and repetitively, enabling the characterisation of the acute dynamic response of leaf physiology to abscission. This approach has enabled the rapid assessment of several novel physiological characteristics, including the RWC at the end of the WWR and the RWC_{gs50}. Further, these characteristics are measured directly in the same leaf, hence the dynamics between stomatal conductance and leaf water content are more closely aligned both spatially and temporally, than by regression from more disparate, stochastic measures taken along a dehydration gradient commonly used to assess stomatal sensitivity for example (Bourne et al., 2017; Dayer et al., 2020).

4.1 | The IRGA and NMR estimates of leaf RWC were closely aligned over the drydown

The reference curves constructed from many leaves and over a range of hydrated states confirmed that the NMR signal estimated

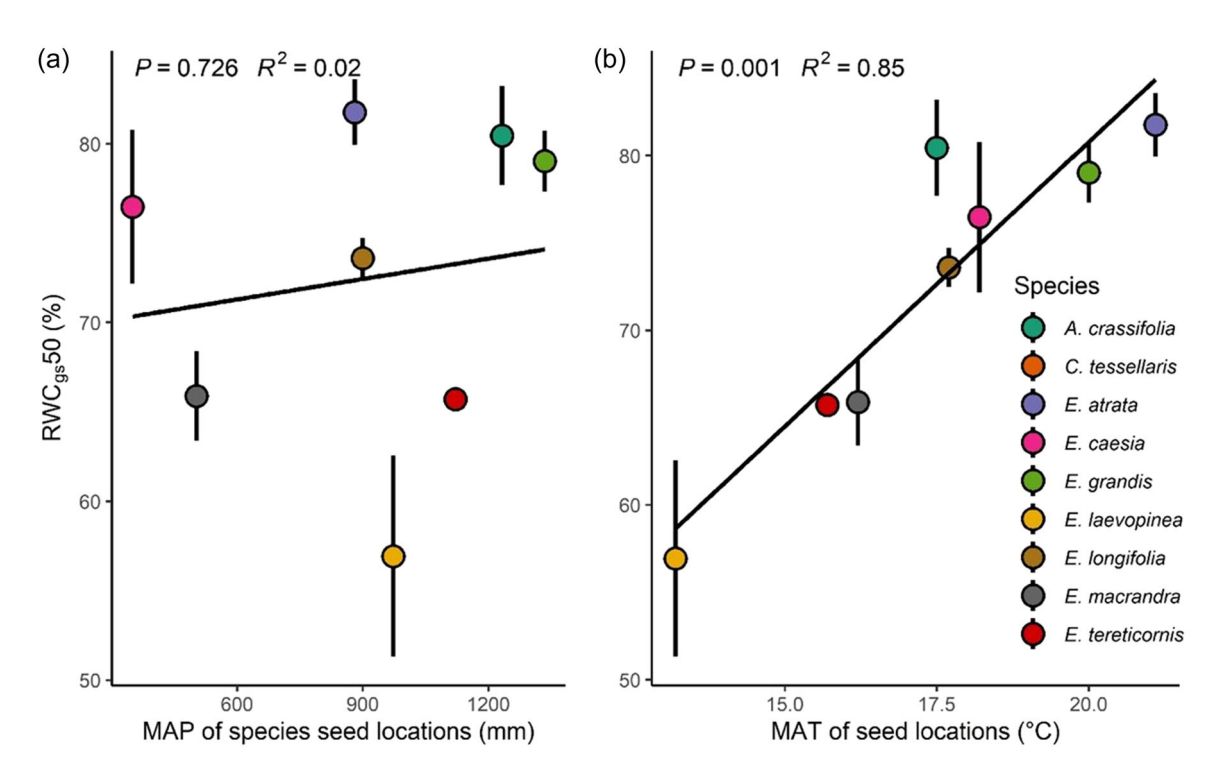


FIGURE 5 The RWC at 50% stomatal conductance plotted against (a) mean annual precipitation and (b) mean annual temperature ($^{\circ}$ C) of the seed collection locations for eight species of eucalypt. n = 4 (note n = 3 for *Eucalyptus caesia* and *Eucalyptus tereticornis*). [Color figure can be viewed at wileyonlinelibrary.com]

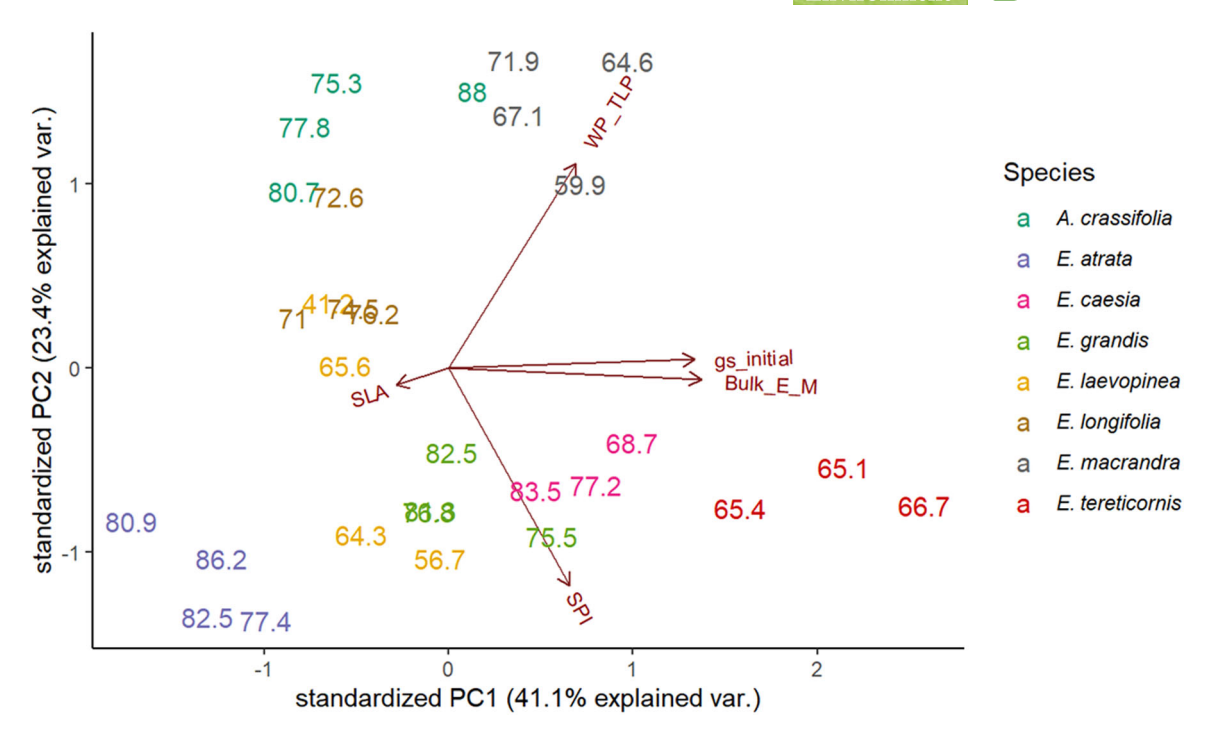


FIGURE 6 Principal component analysis biplot of PCs 1 and 2, among metrics of species physical traits and response to desiccation. Number labels are the RWC at gs₅₀ for each replicate in (%). Eigenvector labels represent the following metrics: gs, initial the rate of stomatal conductance under high light conditions and with the branch connected to a water supply (gs initial, Table 3); bulk_E_M, the bulk elastic modulus (ε, Table 4); SPI, the stomatal pore index (Table 2); WP_TLP, water potential at turgor loss (Ψ_{s,TLP}, Table 4); SLA, specific leaf area (Table 2). [Color figure can be viewed at wileyonlinelibrary.com]

the absolute mass of water in the leaf, and consequently the RWC with a high level of confidence (Figure 3a and Supporting Information: Figure \$1). Despite the agreement between the estimates of RWC dynamics of the IRGA and NMR in leaves isolated from the branch (Figure 3b), there appeared to be subtle differences in acceleration and deceleration of the NMR RWC which were not observed in the IRGA data. This may be due to uneven rates of drying across the leaf surface, caused by factors such as differences in the amount of the light across the surface of the leaf inside the cuvette, from loss of hydraulic connectivity and/ or cavitation of major conduits such as the midvein or from subtle shifts in volume of tissue within the field of view due to leaf shrinkage. An alternative explanation is that the portion of the leaf inside the NMR field from which the leaf RWC was derived, was the widest part of the leaf and would decline at a faster rate than the average leaf surface area. A caveat of this method of validation is the rate at which drying occurs. In the experimental replicates, we deliberately chose to provide the leaf with an additional source of water from branch tissues so as to slow leaf water loss. It is likely that more gradual rates of drying (compared to when only applied to a leaf) would reduce the observed discrepancy between the two technologies, rather than exacerbate it. Nevertheless, the strong linear relationship between NMR signal and mass of water in the leaf allowed us to confidently estimate the stomatal conductance at a range of biologically meaningful leaf water contents over the drydown.

RWC at g_s50 and MAT of the environmental origins are linearly correlated—an ecophysiological measure of stomatal response to bulk leaf RWC

Leaf RWC₉₅₅₀ correlated linearly to the MAT at the seed location of origin for each species. Species from warmer climates closed stomata at higher RWCs than those adapted to cooler climates, suggesting that species from warmer climates possess a greater capacity to respond to rapid changes in abiotic conditions, such as in the dry down experiment. Our study represents the first interspecies characterisation of RWC_{gs50} in vivo, using a technique that empirically measures this property via continuous measurement of both g_s and RWC. The linear relationship of leaf hydraulic status with MAT is consistent with the observation that in Corymbia callophylla hydraulic vulnerability varies with the climate of origin MAT of sites across the species climatic range (Blackman et al., 2017). This suggests that the effect of climate of origin on the ability to tolerate hydraulic stress varies within a species across a local area, as well as interspecifically among species spanning diverse climates and regions across the Australian continent. This kind of trait distribution across and within species in a continuum is also seen in other hydraulic parameters such as the extent of iso and anisohydry (Li et al., 2019) and drought mortality risk factors (Martinez-Vilalta et al., 2019).

In studies that have investigated similar questions of stomatal response to hydraulic status in eucalypts, relationships between stomatal sensitivity and environmental variables representative of

.3653040, 2023, 12, Downloaded

- Davis

home climate have been detected, although the latter variables were representative of water availability and aridity rather than temperature (Bourne et al., 2015; Li et al., 2018). This may be due to differences in methodology and terminology used to describe these parameters. For example, Bourne et al. (2017) defined gs50 as the water potential at which leaves reached 50% of maximum stomatal conductance of all leaves in that species. Climate indicators such as MAP used in this study were derived from the mean across the occurrence range of species, while in the current work we adopted the climate indices at the geographic coordinates of where the seed was collected. But perhaps the largest difference between the methodologies derives from the experimental treatment of the leaf over the drydown. Whilst the leaves used to determine the gs50 parameter in studies such as Bourne et al. (2017) may experience many different levels of light over the drydown period, including low light conditions of a laboratory benchtop, leaves in our study experience uniform, high light conditions for the duration of the drydown over many hours; the only variable changing over that time being the water content of the leaf. Thus our data are measuring a somewhat different properties of the leaf stomatal response.

Our metric of stomatal sensitivity, RWC_{gs50}, did not correlate with rainfall (MAP), a fact which suggests that VPDL, rather than water availability alone was a determining factor. VPD₁ is considered one of the major driving forces behind changes in stomatal aperture and increases exponentially with air temperature (Grossiord et al., 2020). Three parameters determine VPD_L, air temperature (T_A) , leaf temperature (T_I) and relative humidity of the air (RH). T_I in relation to T_A is modulated in species of eucalypts via a number of physical properties including leaf angle and reflectance (Ball et al., 1988; King, 1997), while the mean annual relative humidities (MARH) at the climates of origin of the species in this study (with the exception of E. caesia, 57.2%) are guite similar (67.5%-72.5%). Over the temperature range relevant to species in this study (~8-40°C) and assuming a similar MARH of 70%, the relationship between VPD₁ and air temperature could be constrained to vary almost linearly with only a modest buffering in leaf temperatures, averaged across both time and spatial scales (Supporting Information: Figure S2). We thus interpret the MAT as varying proportionally with VPD_L and determining the RWC at which stomata close in response to severe hydraulic stress. Even E. caesia, with a MARH ~10% lower than other species, has an RWC₉₅₅₀ closely aligned to the linear trend with MAT. The strong linear relationship between RWC_{ss50} and MAT may likely present a useful environmental indicator for how plants may respond to future climate scenarios (Grossiord et al., 2020) and for our capacity to characterise and predict tree survival out of their natural environmental range.

Which leaf traits account for variation in RWC₉₅₅₀? The combination of stomatal traits (gs initial, SPI), water potential metrics $(\Psi_{\mathsf{TLP}}, \varepsilon)$ and leaf physical characteristics (SLA) measured in this study accounted for roughly two-thirds of the variation in RWC₉₅₅₀ (Figure 6). A similar complex interplay of traits influencing Ψ_{gs50} was found among species from California (Henry et al., 2019), who found evidence for a tradeoff between maximum stomatal

conductance and Ψ_{gs50} , which could be explained by stomatal size and densities, SLA and other leaf characteristics. Similarly, additional traits such as the limitations of osmotic control of guard cells, hydraulic connectivity and partitioning of water stores across branch and leaf anatomy would modulate the successful closure of stomata in response to sudden severe hydraulic stress.

A. crassifolia leaves closed their stomata at much higher RWCs than plants of similar climate of origin MATs. This is likely caused by a combination of ecophysiological leaf properties known to govern stomatal closure (Brodribb & Holbrook, 2003) and branch morphological properties or most likely, a combination of both (López et al., 2021). A low initial Ψ_{gs50} may have reduced the severity of the stress response initially and allowed for early stomatal closure. It is also possible that A. crassifolia enacts an exaggerated conservative strategy in response to hydraulic stress to adapt to its native range, limited to a small area of fast-draining shallow soils on sandstone plateaus in the Sydney region (Table 1).

4.3 Despite steadily decreasing leaf RWC. secondary increases in stomatal conductance indicate loss of stomatal control or biophysical resistances to water loss in arid-adapted species

Large increases in g_s after the completion of the WWR, despite declining hydraulic status, were observed in some replicates of at least three of the species in the study, but in particular in two of the four replicates of C. tessellaris (Figure 4). There are two likely explanations for this phenomenon. First, this 'secondary' WWR may point to an interruption in the coordination of guard cell osmoregulation with turgor in the surrounding epidermal cells. It is not clear why the stomatal closure response was reversed in these leaves, however, this secondary WWR was present in species with comparatively high ε . When the value of ε is high, a small decrease in RWC can lead to a large decrease in water potential (Turner, 1988), perhaps increasing the likelihood of water potential in the epidermis outpacing or fatally damaging the guard cell osmoregulation process. Alternatively, it is possible that the secondary WWR represents changes in total leaf surface conductance resulting from structural failure of epidermal cells and/or cuticle, rather than changes in stomatal aperture. The subsequent decline in apparent g_s could then reflect the steep decline in water availability within the leaf, which would render temperature-based estimation of the evaporative gradient invalid.

We also observed smaller, more transient increases in conductance of particular leaves during the decline in RWC (e.g., Figure 4e, E. grandis at ~100 min and E. caesia at ~150 min). These transient increases may be caused by oscillations of g_s (Figure 4). In the course of attaining an appropriate equilibrium of g_s with leaf RWC, the rate of conductance seemed to briefly 'overcorrect', before continuing to decline during the next oscillation cycle. Similar patterns in the g_s response to hydraulic decline have been observed in Vicia faba (Assmann & Gershenson, 1991). Our data shows that overcorrection

can occur either due to large water stores in the leaf that can buffer against water loss (perhaps in the case of E. caesia) or due to the rapidity of closure exceeding the rate of water loss (likely the dominating effect in E. grandis). Both kinds of secondary increases were unpredictable or not replicable from our data but may still be of importance. They provide a possible explanation that would contribute to larger than expected error ranges in studies measuring the K_{leaf} response to declining RWC (Blackman et al., 2017; Bourne et al., 2017; Hernandez-Santana et al., 2016). Multiple methodological approaches to the determination of K_{leaf} (Flexas et al., 2013) assume (i) stomatal closure response to declining hydraulic status is unidirectional and relatively similar between each leaf (e.g., the evaporative flux method) and (ii) that having applied hydraulic stress to a leaf via excision, the mechanisms governing stomatal function remain intact to measure the g_s during rehydration (dynamic kinetic rehydration method). Our data shows that at least in some replicates this is not the case.

4.4 | Interpreting leaf RWC at the end of the WWR —a measure of short-term stomatal response to leaf water content

Our eucalypt leaves, drying down while still attached to cut branches had longer WWR times (30–117 min), to those observed in other woody tree species measured on both intact leaves exposed to sudden increases in VPD and on severed leaves (25–45 min) (Buckley et al., 2011; Kaiser & Paoletti, 2014; Powell et al., 2017; Powles et al., 2006). The longest WWR times reported in the literature are of woody tree and shrub species such as *Umbellularia californica* and *Olea europaea* and plants grown in field conditions as opposed to controlled environments, which supports long WWR for these field grown eucalypts.

Further to previous investigations reporting WWR times, this study is the first to report leaf RWC at the completion of the WWRthat is, a water status metric at which species were able to regain stomatal control following a reduction in bulk leaf RWC. This study shows that for most species of eucalypt the WWR was completed at RWCs well below the RWC_{TLP}, a physiologically critical hydraulic threshold (Tables 2 and 4), thought to correlate with stomatal closure and with drought resilience. There are at least two possible scenarios which could contribute to the long WWR times and the leaf experiencing RWC below TLP before stomatal closure commenced. Firstly, the rapidity of dehydration imposed on leaves in this branch drydown method may impede the ability of stomata to initiate closure at the rate required to preserve a high RWC. Induction of ABA synthesis or solute unloading from the guard cells may not be adequate to overcome the sudden loss of turgor in the epidermis surrounding guard cells for some time, by which time the RWC_{TLP} is already exceeded. Secondly, leaves of some eucalypt species may reach RWCs well below their TLP regularly in their natural environment, and thus may have adapted to delay stomatal closure

until RWC is well below TLP. The occurrence of physiological function below TLP has been discussed previously (Blackman, 2018; Farrell et al., 2017; Zhu et al., 2018) and suggests an important role, particularly among genera from dry environments (Farrell et al., 2017) as is the case for the present study. In a natural environment, the leaf would only experience this hydraulically stressful state momentarily, as the closure of stomata would normally cause the leaf to rapidly refill with water supplied by an intact hydraulic connection to the soil; that connection was, by design, severed in our experiments. Evidence for the second scenario is also found in the WWR metrics of E. atrata. The WWR lasted an average of 55 min for this species and the RWC reached 10% RWC below the TLP before stomatal closure was initiated. Surprisingly, stomata of leaves of this species were able to fully close and maintain leaf RWCs above 50% for more than 10 h in full light conditions (Figure 4). We interpret the resilience of E. atrata leaves in the face of physiologically low RWCs as evidence to suggest that leaves of species originating from environments where water is commonly limiting, are physiologically active often below their TLP. This observation has been hypothesised before (Franks et al., 2007) and has been observed in other eucalypts. For example, Brodribb et al. (2016) demonstrated Eucalyptus globulus, a mesic species, to close stomata post-TLP in a similar experimental treatment on excised branches. Whilst agreement between studies suggest a common capacity for this response, further investigation, particularly on the water contents and WWR dynamics of in situ field-based leaves will shed light on this important characteristic.

5 | CONCLUSION

Here we demonstrate a novel method combining NMR sensing with leaf gas exchange for the precise, accurate and non-destructive measurement of leaf RWC and g_s. Employing this technique, we reveal the dynamics of stomatal closure in response to water deficit and its differing response among eucalypt species of contrasting environmental origin. The response of g_s to water deficit was nonunidirectional in several species, demonstrating stomatal sensitivity to declining water status as well as a failure of the mechanism governing stomatal control to remain intact during dehydration. We define a novel metric of stomatal closure-RWC_{WWR}-and found it differed between species of eucalypt. This provides evidence for leaves to experience RWCs below TLP to enact stomatal closure. Our data confirms that leaf RWC_{gs50} is a highly conserved and standardising ecological trait with potential for use in rapid phenotyping within and between eucalypt species across a range of environments.

ORCID

REFERENCES

- Albasha, R., Fournier, C., Pradal, C., Chelle, M., Prieto, J.A., Louarn, G. et al. (2019) HydroShoot: a functional-structural plant model for simulating hydraulic structure, gas and energy exchange dynamics of complex plant canopies under water deficit—application to grapevine (Vitis vinifera). In Silico Plants, 1(1), diz007. https://doi.org/10.1093/insilicoplants/diz007
- Van As, H. (2006) Intact plant MRI for the study of cell water relations, membrane permeability, cell-to-cell and long-distance water transport. *Journal of Experimental Botany*, 58(4), 743–756.
- Van As, H., Reinders, J.E.A., de Jager, P.A., van de Sanden, P.A.C.M. & Schaafsma, T.J. (1994) In situ plant water balance studies using a portable NMR spectrometer. *Journal of Experimental Botany*, 45(1), 61–67.
- Assmann, S.M. & Gershenson, A. (1991) The kinetics of stomatal responses to VPD in Vicia faba: electrophysiological and water relations models. Plant, Cell & Environment, 14(5), 455–465.
- Ball, M., Cowan, I. & Farquhar, G. (1988) Maintenance of leaf temperature and the optimisation of carbon gain in relation to water loss in a tropical mangrove forest. Functional Plant Biology, 15(2), 263–276.
- Blackman, C.J. (2018) Leaf turgor loss as a predictor of plant drought response strategies. *Tree Physiology*, 38(5), 655–657.
- Blackman, C.J., Aspinwall, M.J., Tissue, D.T. & Rymer, P.D. (2017) Genetic adaptation and phenotypic plasticity contribute to greater leaf hydraulic tolerance in response to drought in warmer climates. *Tree Physiology*, 37(5), 583–592.
- Blackman, C.J., Brodribb, T.J. & Jordan, G.J. (2009) Leaf hydraulics and drought stress: response, recovery and survivorship in four woody temperate plant species. *Plant*, *Cell & Environment*, 32(11), 1584–1595.
- Boland, D.J., Brooker, M.I.H., Chippendale, G., Hall, N., Hyland, B. & Johnston, R.D. et al. (2006) Forest trees of Australia. CSIRO publishing.
- Borchers, H.W. & Borchers, M.H.W. (2019) Package 'pracma'.
- Borisjuk, L., Rolletschek, H. & Neuberger, T. (2012) Surveying the plant's world by magnetic resonance imaging. *The Plant Journal*, 70(1), 129–146
- Bourne, A.E., Creek, D., Peters, J.M.R., Ellsworth, D.S. & Choat, B. (2017) Species climate range influences hydraulic and stomatal traits in *Eucalyptus* species. *Annals of Botany*, 120(1), 123–133.
- Bourne, A.E., Haigh, A.M. & Ellsworth, D.S. (2015) Stomatal sensitivity to vapour pressure deficit relates to climate of origin in *Eucalyptus* species. *Tree Physiology*, 35(3), 266–278.
- Brodribb, T.J., Bienaimé, D. & Marmottant, P. (2016) Revealing catastrophic failure of leaf networks under stress. *Proceedings of the National Academy of Sciences*, 113(17), 4865–4869.
- Brodribb, T.J. & Holbrook, N.M. (2003) Stomatal closure during leaf dehydration, correlation with other leaf physiological traits. *Plant Physiology*, 132(4), 2166–2173.
- Browne, M., Yardimci, N.T., Scoffoni, C., Jarrahi, M. & Sack, L. (2020) Prediction of leaf water potential and relative water content using terahertz radiation spectroscopy. *Plant Direct*, 4(4), e00197.
- Buckley, T.N. (2019) How do stomata respond to water status? New *Phytologist*, 224(1), 21–36.
- Buckley, T.N., John, G.P., Scoffoni, C. & Sack, L. (2015) How does leaf anatomy influence water transport outside the xylem? *Plant Physiology*, 168(4), 1616–1635.
- Buckley, T.N., Sack, L. & Gilbert, M.E. (2011) The role of bundle sheath extensions and life form in stomatal responses to leaf water status. *Plant Physiology*, 156(2), 962–973.
- Dayer, S., Herrera, J.C., Dai, Z., Burlett, R., Lamarque, L.J., Delzon, S. et al. (2020) The sequence and thresholds of leaf hydraulic traits underlying grapevine varietal differences in drought tolerance. *Journal of Experimental Botany*, 71(14), 4333–4344.

- Edwards, C., Sanson, G.D., Aranwela, N. & Read, J. (2000) Relationships between sclerophylly, leaf biomechanical properties and leaf anatomy in some Australian heath and forest species. *Plant Biosystems-An International Journal Dealing with all Aspects of Plant Biology*, 134(3), 261–277.
- Fahn, A. & Broido-Altman, S. (1990) Plant anatomy. Pergamon Press.
- Farrell, C., Szota, C. & Arndt, S.K. (2017) Does the turgor loss point characterize drought response in dryland plants? *Plant, Cell & Environment*, 40(8), 1500–1511.
- Flexas, J., Scoffoni, C., Gago, J. & Sack, L. (2013) Leaf mesophyll conductance and leaf hydraulic conductance: an introduction to their measurement and coordination. *Journal of Experimental Botany*, 64(13), 3965–3981.
- Franks, P.J., Drake, P.L. & Froend, R.H. (2007) Anisohydric but isohydrodynamic: seasonally constant plant water potential gradient explained by a stomatal control mechanism incorporating variable plant hydraulic conductance. *Plant, Cell & Environment*, 30(1), 19–30.
- Gente, R., Rehn, A., Probst, T., Stübling, E.-M., Camus, E.C., Covarrubias, A.A. et al. (2018) Outdoor measurements of leaf water content using THz quasi time-domain spectroscopy. *Journal of Infrared, Millimeter, and Terahertz Waves*, 39(10), 943–948.
- Grossiord, C., Buckley, T.N., Cernusak, L.A., Novick, K.A., Poulter, B., Siegwolf, R.T.W. et al. (2020) Plant responses to rising vapor pressure deficit. New Phytologist, 226(6), 1550–1566.
- Henry, C., John, G.P., Pan, R., Bartlett, M.K., Fletcher, L.R., Scoffoni, C. et al. (2019) A stomatal safety-efficiency trade-off constrains responses to leaf dehydration. *Nature Communications*, 10(1), 3398.
- Hernandez-Santana, V., Rodriguez-Dominguez, C.M., Fernández, J.E. & Diaz-Espejo, A. (2016) Role of leaf hydraulic conductance in the regulation of stomatal conductance in almond and olive in response to water stress. *Tree Physiology*, 36(6), 725–735.
- Huber, A.E., Melcher, P.J., Piñeros, M.A., Setter, T.L. & Bauerle, T.L. (2019) Signal coordination before, during and after stomatal closure in response to drought stress. New Phytologist, 224(2), 675–688.
- Ivanoff, L. (1928) 32. L. Iwanoff: Zur Methodik der Transpirationsbestimmung am Standort. Berichte der Deutschen Botanischen Gesellschaft, 46, 306–310.
- Jin, X., Shi, C., Yu, C.Y., Yamada, T. & Sacks, E.J. (2017) Determination of leaf water content by visible and near-infrared spectrometry and multivariate calibration in Miscanthus. Frontiers in Plant Science, 8, 721.
- Kaiser, H. & Paoletti, E. (2014) Dynamic stomatal changes, *Trees in a changing environment*. Springer, pp. 61–82.
- King, D.A. (1997) The functional significance of leaf angle in Eucalyptus. Australian Journal of Botany, 45(4), 619–639.
- Körner, C. & Cochrane, P.M. (1985) Stomatal responses and water relations of *Eucalyptus pauciflora* in summer along an elevational gradient. *Oecologia*, 66(3), 443–455.
- Lechthaler, S., Robert, E.M.R., Tonné, N., Prusova, A., Gerkema, E., Van As, H. et al. (2016) Rhizophoraceae mangrove saplings use hypocotyl and leaf water storage capacity to cope with soil water salinity changes. Frontiers in Plant Science, 7, 895. https://doi.org/10. 3389/fpls.2016.00895
- Li, X., Blackman, C.J., Choat, B., Duursma, R.A., Rymer, P.D., Medlyn, B.E. et al. (2018) Tree hydraulic traits are coordinated and strongly linked to climate-of-origin across a rainfall gradient. *Plant, Cell & Environment*, 41(3), 646–660.
- Li, X., Blackman, C.J., Peters, J.M.R., Choat, B., Rymer, P.D., Medlyn, B.E. et al. (2019) More than iso/anisohydry: hydroscapes integrate plant water use and drought tolerance traits in 10 eucalypt species from contrasting climates. *Functional Ecology*, 33(6), 1035–1049.
- López, R., Cano, F.J., Martin-StPaul, N.K., Cochard, H. & Choat, B. (2021) Coordination of stem and leaf traits define different strategies to regulate water loss and tolerance ranges to aridity. *New Phytologist*, 230(2), 497–509.

ditions) on Wiley Online Library for rules of use; OA articles are governed by the applicable Creative



- Lucani, C., Brodribb, T., Jordan, G. & Mitchell, P. (2018) Intraspecific variation in drought susceptibility in *Eucalyptus globulus* is linked to differences in leaf vulnerability. *Functional Plant Biology*, 46(3), 286–293. https://doi.org/10.1071/FP18077
- Martinez-Vilalta, J., Anderegg, W.R.L., Sapes, G. & Sala, A. (2019) Greater focus on water pools may improve our ability to understand and anticipate drought-induced mortality in plants. New Phytologist, 223(1), 22–32.
- de Mendiburu, F. & de Mendiburu, M.F. (2020) Package 'agricolae'. R package version: 1.2-8.
- Merchant, A., Callister, A., Arndt, S., Tausz, M. & Adams, M. (2007) Contrasting physiological responses of six *Eucalyptus* species to water deficit. *Annals of Botany*, 100(7), 1507–1515.
- Merchant, A., Smith, M.R. & Windt, C.W. (2022) In situ pod growth rate reveals contrasting diurnal sensitivity to water deficit in *Phaseolus vulgaris*. *Journal of Experimental Botany*, 73(11), 3774–3786.
- Merchant, A. (2014) The regulation of osmotic potential in trees. In: Tausz, M. & Grulke, N. (Eds.) *Trees in a changing environment: ecophysiology, adaptation, and future survival.* Dordrecht: Springer Netherlands, pp. 83–97.
- Pau, G., Fuchs, F., Sklyar, O., Boutros, M. & Huber, W. (2010) EBImage—an R package for image processing with applications to cellular phenotypes. *Bioinformatics*, 26(7), 979–981.
- Powell, T.L., Wheeler, J.K., Oliveira, A.A.R., Costa, A.C.L., Saleska, S.R., Meir, P. et al. (2017) Differences in xylem and leaf hydraulic traits explain differences in drought tolerance among mature Amazon rainforest trees. Global Change Biology, 23(10), 4280–4293.
- Powles, J.E., Buckley, T.N., Nicotra, A.B. & Farquhar, G.D. (2006) Dynamics of stomatal water relations following leaf excision. *Plant*, *Cell & Environment*, 29(5), 981–992.
- R Core Team. (2019) R: a language and environment for statistical computing. R Foundation for Statistical Computing, 2020.
- Sack, L., Cowan, P., Jaikumar, N. & Holbrook, N. (2003) The 'hydrology' of leaves: co-ordination of structure and function in temperate woody species. Plant, Cell & Environment, 26(8), 1343–1356.
- Sack, L. & Holbrook, N.M. (2006) Leaf hydraulics. *Annual Review of Plant Biology*, 57(1), 361–381.
- Sack, L. & Scoffoni, C. (2012) Measurement of leaf hydraulic conductance and stomatal conductance and their responses to irradiance and dehydration using the evaporative flux method (EFM). *Journal of Visualized Experiments*, (70), e4179. https://doi.org/10.3791/4179
- Sack, L. & Tyree, M. T. (2005) Leaf hydraulics and its implications in plant structure and function. *Vascular transport in plants*. Academic Press, pp. 93–114.
- Schindelin, J., Arganda-Carreras, I., Frise, E., Kaynig, V., Longair, M., Pietzsch, T. et al. (2012) Fiji: an open-source platform for biological-image analysis. *Nature Methods*, 9(7), 676–682.
- Scoffoni, C., Albuquerque, C., Cochard, H., Buckley, T.N., Fletcher, L.R., Caringella, M.A. et al. (2018) The causes of leaf hydraulic vulnerability and its influence on gas exchange in *Arabidopsis* thaliana. Plant Physiology, 178(4), 1584–1601.
- Scoffoni, C. & Sack, L. (2017) The causes and consequences of leaf hydraulic decline with dehydration. *Journal of Experimental Botany*, 68(16), 4479-4496.
- Team RStudio. (2015) RStudio: integrated development for R, 42. RStudio Inc., p. 14.

- Thornhill, A.H., Crisp, M.D., Külheim, C., Lam, K.E., Nelson, L.A., Yeates, D.K. et al. (2019) A dated molecular perspective of eucalypt taxonomy, evolution and diversification. Australian Systematic Botany, 32(1), 29–48.
- Trueba, S., Pan, R., Scoffoni, C., John, G.P., Davis, S.D. & Sack, L. (2019) Thresholds for leaf damage due to dehydration: declines of hydraulic function, stomatal conductance and cellular integrity precede those for photochemistry. New Phytologist, 223(1), 134–149.
- Turner, N.C. (1988) Measurement of plant water status by the pressure chamber technique. *Irrigation Science*, 9, 289–308.
- Tyree, M.T. & Hammel, H.T. (1972) The measurement of the turgor pressure and the water relations of plants by the pressure-bomb technique. *Journal of Experimental Botany*, 23(1), 267–282.
- Villanueva, R.A.M. & Chen, Z.J. (2019) ggplot2: elegant graphics for data analysis. Taylor & Francis.
- Warren, C.R., Dreyer, E., Tausz, M. & Adams, M.A. (2006) Ecotype adaptation and acclimation of leaf traits to rainfall in 29 species of 16-year-old *Eucalyptus* at two common gardens. *Functional Ecology*, 20(6), 929-940.
- White, D.A., Turner, N.C. & Galbraith, J.H. (2000) Leaf water relations and stomatal behavior of four allopatric *Eucalyptus* species planted in Mediterranean southwestern Australia. *Tree Physiology*, 20(17), 1157–1165.
- Windt, C.W. & Blumler, P. (2015) A portable NMR sensor to measure dynamic changes in the amount of water in living stems or fruit and its potential to measure sap flow. *Tree Physiology*, 35(4), 366–375.
- Windt, C.W., Nabel, M., Kochs, J., Jahnke, S. & Schurr, U. (2021) A mobile NMR sensor and relaxometric method to non-destructively monitor water and dry matter content in plants. Frontiers in Plant Science, 12(18), 617768. https://doi.org/10.3389/fpls.2021.617768
- Windt, C.W., Soltner, H., Dusschoten, D. & Blümler, P. (2011) A portable Halbach magnet that can be opened and closed without force: the NMR-CUFF. *Journal of Magnetic Resonance*, 208(1), 27–33.
- Zhu, S.-D., Chen, Y.-J., Ye, Q., He, P.-C., Liu, H., Li, R.-H. et al. (2018) Leaf turgor loss point is correlated with drought tolerance and leaf carbon economics traits. *Tree Physiology*, 38(5), 658–663.
- Zwieniecki, M.A., Brodribb, T.J. & Holbrook, N.M. (2007) Hydraulic design of leaves: insights from rehydration kinetics. *Plant*, *Cell* & *Environment*, 30(8), 910–921.

SUPPORTING INFORMATION

Additional supporting information can be found online in the Supporting Information section at the end of this article.

How to cite this article: Coleman, D., Windt, C.W., Buckley, T.N. & Merchant, A. (2023) Leaf relative water content at 50% stomatal conductance measured by noninvasive NMR is linked to climate of origin in nine species of eucalypt. *Plant*, *Cell & Environment*, 46, 3791–3805.

https://doi.org/10.1111/pce.14700